Direct versus delayed pathways in strong-field non-sequential double ionization

Direct versus delayed pathways in strong-field non-sequential double ionization

2011 New J. Phys. 13 043001

(http://iopscience.iop.org/1367-2630/13/4/043001)

New Journal of Physics
The open-access journal for physics

Direct versus delayed pathways in strong-field non-sequential double ionization

A Emmanouilidou[1,2,4], J S Parker[3], L R Moore[3] and K T Taylor[3]

[1] Department of Physics and Astronomy, University College London, Gower Street, London WC1E 6BT, UK
[2] Chemistry Department, University of Massachusetts at Amherst, Amherst, MA 01003, USA
[3] DAMTP, Queen's University Belfast, Belfast BT7 1NN, UK
E-mail: a.emmanouilidou@ucl.ac.uk

New Journal of Physics **13** (2011) 043001 (10pp)
Received 6 September 2010
Published 4 April 2011
Online at http://www.njp.org/
doi:10.1088/1367-2630/13/4/043001

Abstract. We report full-dimensionality quantum and classical calculations of the double ionization (DI) of laser-driven helium at 390 nm. Good agreement between the quantum and classical results is observed. We identify the relative importance of the two main non-sequential DI pathways: the direct—with an almost simultaneous ejection of both electrons—and the delayed. We find that the delayed pathway prevails at small intensities independently of total electron energy, but at high intensities the direct pathway predominates up to a certain upper limit in total energy, which increases with intensity. An explanation of this increase with intensity is provided.

Contents

[4] Author to whom any correspondence should be addressed.

1. Introduction

Double ionization (DI) of the He atom when driven by strong laser fields serves as a prototype for exploring correlated electron dynamics in strong fields and has thus been the subject of many studies in recent decades (see [1, 2]). For large intensities of the laser field, the two electrons are stripped out sequentially—sequential DI (SDI) [3]. For smaller intensities, non-sequential DI (NSDI) dominates, resulting in the ejection of strongly correlated electron pairs.

Focusing on the range of intensities corresponding to NSDI, an accepted mechanism yielding DI is provided by the three-step model [4]: (i) an electron escapes through the field-lowered Coulomb barrier, (ii) it moves in the strong infrared laser field and (iii) it returns to the core (possibly multiple times) for transferring energy to the other electron remaining in He^+. Strong support for the three-step model has been provided by both theory [5]–[8] and experiment [9]–[11]. The transfer of energy in step 3 takes place through two main pathways: direct—also referred to as simultaneous ejection (SE); and delayed—also referred to as recollision-induced excitation with subsequent field ionization (RESI) [12, 13]—with a delay in ionization of approximately one-quarter of a laser period or more.

Currently, there is still a lack of understanding of how the relative importance of the direct and delayed DI events depends on the laser intensity and total electron energy. (Throughout this work, the total electron energy we refer to is the sum of the final kinetic energies of the two electrons.) In this work, we show that the delayed pathway prevails for small intensities independently of total electron energy but, in contrast, at high intensities the SE pathway predominates up to an upper limit in total energy—we call this the SE upper limit (SEUL). The SEUL shifts upwards with increasing intensity. We find that accurately accounting for the interaction with the nucleus is crucial for explaining this upward shift.

2. Double ionization (DI) probability distribution: quantum versus classical

The first finding we report in figure 1 is the surprisingly good agreement over an important range of 390 nm laser intensities between our classical results and full-dimensionality quantum ones for helium DI energy spectra. The total energy in figure 1 is expressed in units of ponderomotive energy, $U_p = E_0^2/(4\omega^2)$, a natural choice when comparing different intensities. The laser intensity range considered is important because at 9 (12) $\times 10^{14}$ W cm^{-2} the maximum return energy of the recolliding electron ($3.2U_p$ within the simplest three-step model [4]) equals the first excitation (ionization) energy of ground state He^+.

The laser pulse used in the classical calculations is $E(t) = E_0(t)\cos(\omega t)$ and is linearly polarized along the z-axis. The pulse envelope is defined as $E_0(t) = E_0$ (a constant) for $0 < t < 6\,T$ and $E_0(t) = E_0 \cos^2(\omega(t - 6T)/12)$ for $6T < t < 9T$, with T being the period of the field. The quasiclassical model we use [14] entails electron tunneling through the field-lowered Coulomb potential with a quantum tunneling rate given by the ADK formula [15]. The longitudinal momentum is zero, while the transverse one is given by a Gaussian distribution. The remaining electron is modelled by a microcanonical distribution [16]. Our three-dimensional classical technique employs regularized coordinates [17] to fully account for the Coulomb singularity, resulting in a faster and more stable numerical propagation. This is a major advantage of our classical technique over others that soften the Coulomb potential. The latter cannot accurately describe DI phenomena related to strong interaction with the nucleus and thus cannot account for most of the detailed findings in the present work. Regarding the quantum

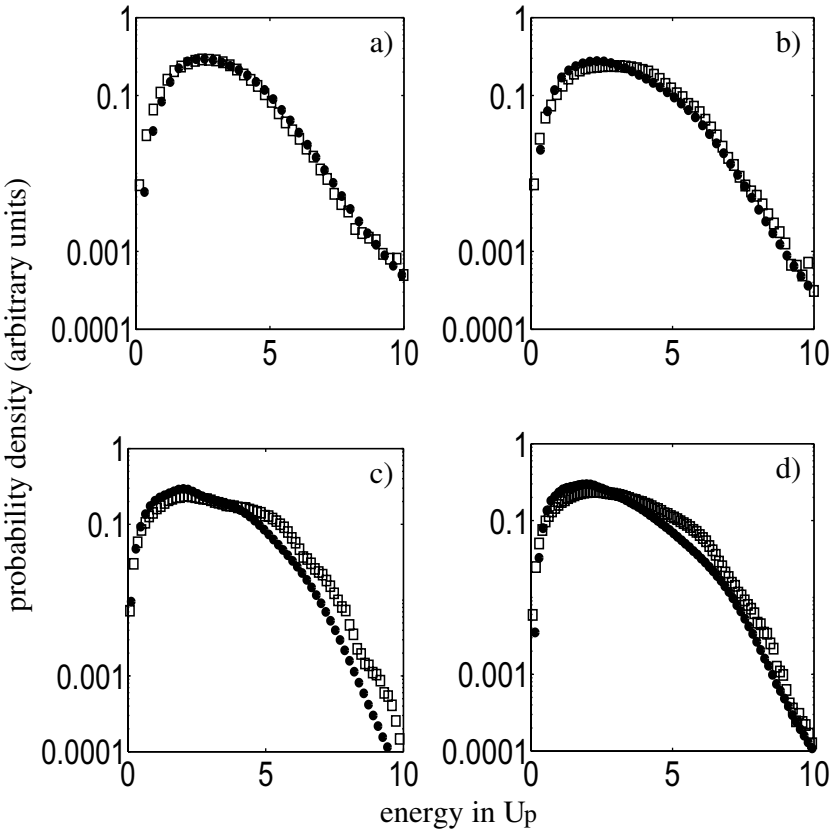

Figure 1. DI probability distributions for a laser pulse of 390 nm with different intensities: (a) 7×10^{14} (b) 9×10^{14} (c) 13×10^{14} and (d) 16×10^{14} W cm^{-2}. The area under each curve is equal to one. The 'smoothed' quantum results are denoted by black circles, whereas the classical ones are denoted by open black squares.

calculation, the time-dependent numerical integration (TDNI) is a finite-difference solution of the full two-electron Schrödinger equation for the helium atom [3]. The TDNI method contains no arbitrarily adjustable parameters: the quality of the numerical solutions is limited by available computational power rather than by ad hoc approximations introduced into the model of the helium atom. In the present calculations, the finite-difference grid point spacings are 0.29 Bohr, and the maximum total angular momentum of the basis set of partial waves (coupled spherical harmonics) is $44\hbar$. The integration volume is a sphere of radius 1200 Bohr. A large integration volume is essential. Reflection of the wavefunction at the boundary of the integration volume gives rise to unacceptably large errors in the calculation of the final-state energy spectrum. With these parameter settings, the maximum measured errors in the energies of bound states and autoionizing states are under 0.01 and 0.1%, respectively. The maximum measured error in the lifetimes of autoionizing states is below 1%.

In the quantum calculation, the momentum spectrum of the ejected two-electron wavepacket is obtained by transforming a subset of the final-state wavefunction from configuration to momentum space. The pulse is ramped-off over three field periods (and the integration is allowed to continue field-free for another half-field period) in order to allow

the two doubly ionizing electrons to move away from the atomic nucleus. A free electron with one photon of energy (at 390 nm) travels 26 Bohr during a field period. A hamming window, similar to that used for calculating spectra in signal processing, is multiplied by the wavefunction prior to the Fourier transform. The window zeroes out the wavefunction near the nucleus, and ramps smoothly to unity at some arbitrary radius R. The transformation is repeated with R between 25 and 80 Bohr in order to estimate sensitivity to R. In the present problem, the spectra obtained in this way are highly insensitive to R. On the scale of figure 1, choosing $R = 25$ and $R = 80$ produces nearly the same spectrum, except at small energies E ($E/U_p \sim 1$ or less). In comparison to the $R = 25$ window, the $R = 80$ window removes more of the wavefunction dominated by slow electrons. Unsurprisingly, the spectrum associated with $R = 80$ is observed to be diminished in comparison to the $R = 25$ result (by up to 20%) for small energies ($E/U_p \sim 1$ or less). Because of its simplicity and insensitivity to R, the windowing method is favoured for calculating the higher-energy parts of the final-state kinetic energy spectra, which are of particular relevance to the physics discussed in this paper, but it cannot be used to obtain high-accuracy DI rates, because some final state population is discarded prior to the Fourier transform. Therefore, a discussion of total DI rates and of discrepancies between classical and quantum DI rates is beyond the scope of this paper. Here we limit the discussion to trends in the energy spectra as a function of energy, and we plot the energy spectra in arbitrary units (figure 1).

The agreement between classical and quantum results is especially surprising on at least two counts. Firstly, the classical approach indeed produces a DI yield at a low laser intensity (7×10^{14} W cm^{-2}), considerably below the collisional excitation threshold intensity of 9×10^{14} W cm^{-2} at 390 nm. DI at such a low laser intensity was long speculated to be either entirely a quantum effect or only possible by means of repeated returns of the recolliding electron to the core. The agreement between classical and quantum results in figure 1 clearly negates the former speculation, and the analysis of classical DI trajectories below will also negate the latter. The second surprise is the agreement over the value of total energy beyond which the DI probability density falls exponentially—in the following, we refer to this energy value as the cut-off. This energy cut-off value increases from $5.2U_p$ at 7×10^{14} W cm^{-2} to about $7.8U_p$ at 13×10^{14} W cm^{-2} in both calculations. Such an increase in the energy cut-off value has previously been reported from the quantum results [19] at this wavelength. The excellent line-up of the classical with the benchmark quantum results in figure 1 strongly motivates us to seek a deeper understanding of the DI process through an analysis of the contributing classical trajectories.

3. DI mechanisms

We identify the two main DI energy transfer classical trajectory pathways by using the time delay between the recollision time and the time of ionization of each electron [20]. We define the recollision time as the time of minimum approach of the two electrons. We identify this time through the maximum in the electron pair potential energy. The ionization time for each electron is defined as the time when the sum of the electron's kinetic energy (using the canonical momentum) and the potential energy due to the electron's interaction with the nucleus becomes positive and remains positive thereafter. For more details of the time of ionization, see [14] and references therein. In the direct ionization pathway (SE) both electrons are ionized simultaneously very close to the recollision time. In the delayed ionization pathway,

Table 1. The percentage contributions, in the given energy regimes, to DI at 7×10^{14}, 9×10^{14} and 13×10^{14} W cm^{-2} from SE, RESIa and RESIb pathways. The energy cut-off has a value of $5.2U_p$, $6.5U_p$ and $7.8U_p$ at these three intensities, respectively.

	SE	RESIa	RESIb
7×10^{14} W cm^{-2}			
Below $5.2U_p$	27.7	14.3	40.9
Above $5.2U_p$	11.4	15.6	64.7
9×10^{14} W cm^{-2}			
Below $5.2U_p$	45.1	12.0	30.4
From $5.2U_p$ to 6.5 U_p	43.9	11.7	39.9
Above $6.5U_p$	12.0	13.2	67.8
13×10^{14} W cm^{-2}			
Below $5.2U_p$	53.4	14.0	24.3
From $5.2U_p$ to $7.8U_p$	62.0	11.6	21.6
Above$7.8U_p$	32.0	15.9	47.0

the recolliding electron excites the remaining electron but does not ionize it. The electron is subsequently ionized at a peak (RESIa) [12, 13] or at a zero (RESIb) [20] of the laser electric field. The relative contribution of the direct and delayed pathways changes as a function of laser intensity. We find that as the intensity increases from 7×10^{14} to 13×10^{14} W cm^{-2}, the contribution of the SE pathway to the total DI yield increases from 25.6 to 53.4%, whereas that of the combined RESIa plus RESIb pathway decreases from 62.0 to 41.8%. Thus, the SE pathway's contribution to total DI prevails for high intensities.

We now focus on the relative contributions of the direct and delayed pathways to DI as well as on the detailed dynamics of the DI pathways for three different intensities within various energy regimes. A convenient way of defining these energy regimes is to use the cut-off energies as boundaries. For each intensity, we consider an upper energy regime bounded from below by the energy cut-off; an intermediate energy regime, if $5.2U_p$ differs from the cut-off energy, bounded from below by $5.2U_p$; and finally a lower-energy regime below $5.2U_p$. As we show below, the effect of the nucleus becomes important at all intensities for energies above $5.2U_p$, thereby justifying our choice of this boundary value. Note that $5.2 = 2 + 3.2$, where $3.2U_p$ is the maximum recollision energy (three-step model) and $2U_p$ is the maximum energy a 'free' electron gains from the laser field.

3.1. Small intensities and the prevalence of the delayed pathway for all total energies

We first consider small intensities, 7×10^{14} W cm^{-2}, where the maximum energy of the recolliding electron $3.2U_p$ in the simplest version of the three-step model is less than the first excitation energy of the ground state of He^+. As shown in table 1, for the smallest intensity considered—7×10^{14} W cm^{-2}—the combined RESIa plus RESIb contribution is the major one in both the energy regimes considered—particularly so in the higher-energy regime above the cut-off.

We next explore the characteristics and general properties of the DI pathways addressed in table 1 by focusing on the momentum component of each electron along the polarization axis

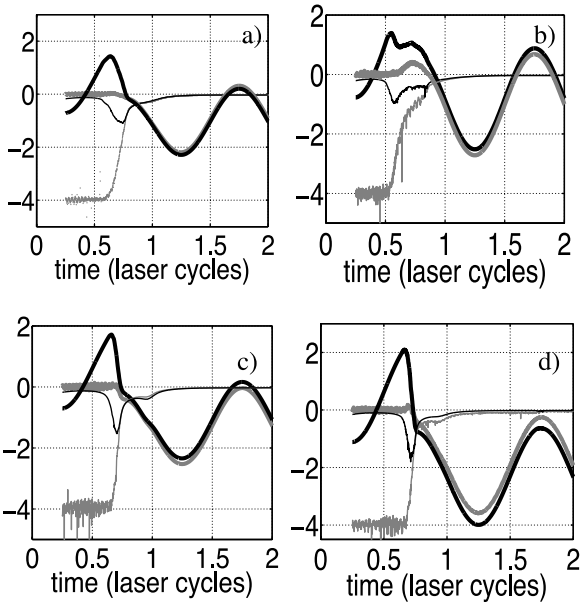

Figure 2. We plot $\langle p_{1,z}\rangle$ (thick black line), $\langle p_{2,z}\rangle$ (thick grey line), $\langle Z/r_1\rangle$ (thin black line) and $\langle Z/r_2\rangle$ (thin grey line). These quantities are shown to scale with the time axis measured in laser cycles. Electron 1 is the recolliding electron, r_i is the distance of electron i from the nucleus, and $Z = 2$. The plotted quantities are shown for the SE pathway, for (a) $7 \times 10^{14}\,\mathrm{W\,cm^{-2}}$ at energies below $5.2U_\mathrm{p}$, (b) $13 \times 10^{14}\,\mathrm{W\,cm^{-2}}$ at energies below $5.2U_\mathrm{p}$, (c) $7 \times 10^{14}\,\mathrm{W\,cm^{-2}}$ at energies above $5.2U_\mathrm{p}$, and (d) $13 \times 10^{14}\,\mathrm{W\,cm^{-2}}$ at energies above $7.8U_\mathrm{p}$.

(the z-axis). We plot for each electron the average of this component, $\langle p_{1,z}\rangle$ and $\langle p_{2,z}\rangle$, for the SE pathway in figure 2 and for the RESIb pathway in figure 3. The time of recollision is the time of minimum distance between the two electrons, identified in figures 2 and 3 as the time at which there is a sudden rise/dip in the nuclear contribution to the potential energy of the second/first electron. In the SE pathway, electron 2 ionizes at a time close to the time of recollision, while in RESIb electron 2 ionizes around $T/2$ later. In both figures 2 and 3, we consider only those trajectories where the recollision occurs at the first return of the recolliding electron to the nucleus. For 390 nm, this is found to be the most important contribution to the SE and RESI pathways for all intensities, even for the low intensity of $7 \times 10^{14}\,\mathrm{W\,cm^{-2}}$. Nevertheless, multiple returns of the recolliding electron are explicitly accounted for in table 1. In addition, the general properties of SE and RESIb pathways for one return of the recolliding electron, described below, hold true for multiple returns—the only difference being the recollision time.

At $7 \times 10^{14}\,\mathrm{W\,cm^{-2}}$, for both energy regimes, the recollision time is very close to $(2/3)T$ in accord with a maximum energy recollision in the simplest version [4] of the three-step model. At the instant of recollision, the recolliding electron in the SE, figures 2(a) and (c), and RESIb, figures 3(a) and (c), pathway first loses energy ($\langle p_{1,z}\rangle$ suddenly decreases) to the second electron. It is then pulled by the field—which in the meantime has changed sign—as well as by the nucleus, in a direction opposite to its incoming direction before recollision. The significant interaction of the recolliding electron with the nucleus is also seen as an almost discontinuous change in $\langle p_{1,z}\rangle$ shortly after $(2/3)T$ in figures 2(a) and (c) and also in figures 3(a) and (c). In

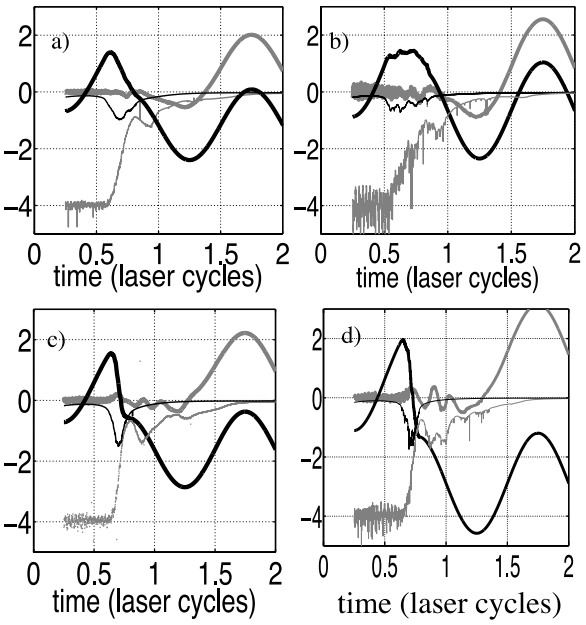

Figure 3. The same as in figure 2 but for the RESIb pathway.

the SE pathway the field also pulls, promptly ionizing electron 2 in the same direction as the recolliding electron's direction after recollision, while for the RESIb pathway, electron 2 ionizes later at the next zero of the field. Even though the interaction of the recolliding electron with the nucleus is more pronounced for total energies above $5.2U_p$, the differences between the two energy regimes are small for both pathways.

3.2. Higher intensities and the prevalence of the delayed pathway only for high total energies

We now consider intensities where the maximum energy of the recolliding electron ($3.2U_p$ in the simplest version of the three-step model) is greater than the first excitation energy of the ground state of He^+. As shown in table 1, at intensities of 9×10^{14} and $13 \times 10^{14}\,W\,cm^{-2}$, the delayed pathway remains the predominant one for energies above the cut-off. However, as the intensity increases from 7×10^{14} to $13 \times 10^{14}\,W\,cm^{-2}$, the contribution of the SE trajectories becomes increasingly more important below the cut-off energy, changing from 27.7 to 62.0%. For the higher intensities in table 1, 9×10^{14} and $13 \times 10^{14}\,W\,cm^{-2}$, it is clear that the SE pathway prevails to an upper limit in energy—the SEUL—which increases with intensity. We show below the crucial role that the nucleus plays in this increase in the SEUL.

3.2.1. Small energies and early recollision time. At higher intensities, the behaviour of $\langle p_{1,z} \rangle$ against time differs markedly as we go from one energy regime to the next, most noticeably so at $13 \times 10^{14}\,W\,cm^{-2}$. For energies below $5.2U_p$, figures 2(b) and 3(b), the interaction of the recolliding electron with the nucleus is small in both pathways. The recollision takes place at a time close to $T/2$ rather than at $(2/3)T$ (the time of maximum energy recollision in the three-step model). At the instant of recollision, the momentum of the recolliding electron first decreases due to transfer of energy to the second electron—dip in $\langle p_{1,z} \rangle$ around $T/2$ in figure 2(b). But at this early recollision time, the laser field does not undergo a sign change and

so continues to pull electron 1 in the same direction as prior to recollision. In the SE pathway, $\langle p_{2,z}\rangle$ has the same sign as $\langle p_{1,z}\rangle$ since ionized electron 2 experiences the same direction of pull from the field as does electron 1. Thus, for high enough intensities within the NSDI regime, SE is similar to a field-free $(e, 2e)$ process for small total energies. This is in agreement with the movie analysis of the two-electron quantum wavepackets [1].

High energies and later recollision time. For the highest-energy regime (see figures 2(d) and 3(d)), the time of recollision for both pathways comes close to $(2/3)T$. The interaction of the recolliding electron with the nucleus is very strong (as indeed is the case both below and above $5.2U_p$ for 7×10^{14} W cm^{-2}). The recolliding electron gets sharply pulled back by both the laser field and the nucleus and reverses in direction, as is the case for small intensities.

To sum up, the SE pathway begins as a small contribution at low intensity, but dominates for high intensities for total energy below the SEUL (see table 1). Below $5.2U_p$, the recollision time is around $T/2$ and the interaction with the nucleus is small, resulting in comparable and small escape energies of the two ionizing electrons. For low intensities and any total energy, as well as high intensity and total energy above the SEUL, the RESI pathway dominates. To achieve high-energy DI (beyond $5.2U_p$ at any laser intensity), the recolliding electron must undergo a strong interaction with the nucleus following a gain of near maximum energy from the laser field—recollision time close to $(2/3)T$. For total energy beyond $5.2U_p$, the energy sharing between the two electrons is quite asymmetric.

3.3. Dependence on intensity of the simultaneous ejection upper limit (SEUL)

We now explore the physical reason for the SEUL shifting to higher U_p values with increasing intensity (see table 1). Firstly, we note that despite this shift, the maximum escape energy of electron 2 remains almost constant at around $2U_p$ [19]. Secondly, for energies below the rising SEUL, the SE pathway's contribution to DI increases from 27.7 to 62.0% with increasing intensity (see table 1). Given these observations, the question boils down to: Why does the final escape energy of electron 1 in the SI pathway increase dramatically, by almost $2.5U_p$, as the intensity increases from 7×10^{14} to 13×10^{14} W cm^{-2}?

For intensities of 7×10^{14} and 13×10^{14} W cm^{-2}, we plot in figure 4 the radial distances (from the nucleus) of electrons 1 and 2 in the SE pathway taking into account only total escape energies extending $1U_p$ below the intensity-dependent cut-off. The time zero in these plots corresponds to the recollision instant. Frames (a) and (b) make clear that at 7×10^{14} W cm^{-2} both electrons escape with about the same speed, but at 13×10^{14} W cm^{-2}, although the electrons escape with higher speeds in line with increasing U_p, the recolliding electron 1 considerably outpaces initially bound electron 2. Insights into how electron 1 gains higher escape energy at 13×10^{14} W cm^{-2} can be gleaned by examining the bottom frames of figure 4, which show magnifications of the top frames at times close to the recollision instant. At 7×10^{14} W cm^{-2}, we observe prior to the recollision that (initially bound) electron 2 has an average distance from the nucleus of 0.5 a.u., as expected for an electron residing in the He^+ ground state. At the instant of recollision, electron 1 has a radial distance larger than this, at around 0.8 a.u. In contrast, at 13×10^{14} W cm^{-2}, we see from figure 4(d) that at the recollision instant electron 1 gets closer to the nucleus than does electron 2. Thus, at 13×10^{14} W cm^{-2}, electron 1 experiences an unscreened nuclear charge, making the role of the nucleus all the greater in controlling this electron and giving it the opportunity to subsequently pick up greater energy from the laser field.

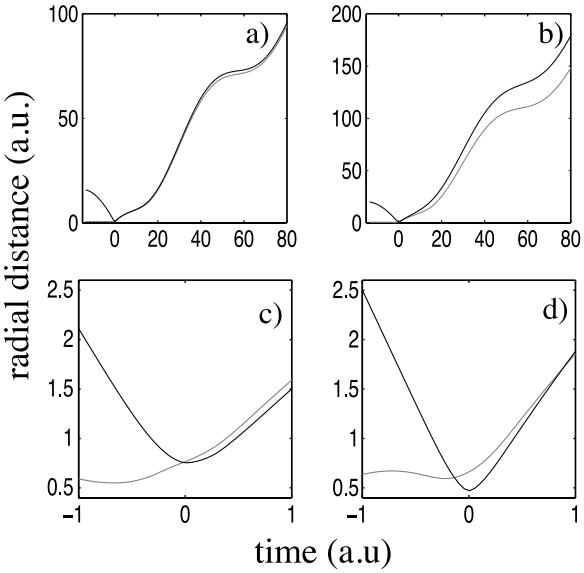

Figure 4. The radial distance of the recolliding electron (black line) and of the initially bound electron (grey line) for the SI pathway for 7×10^{14} W cm^{-2} (left) and 13×10^{14} W cm^{-2} (right) as a function of time for large times (a and b) and small times (c and d). Time zero is the recollision time.

4. Conclusions

We have found surprisingly good agreement between the results from full quantum and classical calculations for DI energy spectra of 390 nm laser-driven helium over an important range of laser intensities. We have analysed the classical results via a unified picture of DI pathways (direct and delayed) and established how their relative preponderances change with intensity and total electron escape energy. We find that the nucleus can play a very important role and that the shift upwards in the SEUL with increasing laser intensity comes about through the ability of the recolliding electron to encounter the unscreened nucleus at higher laser intensity in the direct pathway. We have shown that DI at a low intensity (7×10^{14} W cm^{-2}) is possible in a classical description where it occurs overwhelmingly via the delayed pathway and strong participation of the nucleus. Moreover, an interesting finding of this work is that at 390 nm, at all intensities explored, the recollision at first return of the driven electron dominant in all regions of the DI energy spectra. This is not the case at 800 nm, where our preliminary results show returns—of the recolliding electron to the core—other than the first to be the dominant ones. Future work is needed to understand how the number of returns of the recolliding electron depends on the frequency of the laser pulse.

Acknowledgments

AE acknowledges support through funding from the EPSRC under grant no. EPSRC/H0031771 and from the NSF under grant no. NSF/0855403. The work of the other authors was supported by the EPSRC and by a Cray Centre of Excellence Award.

References

[1] Taylor K T, Parker J S, Dundas D and Meharg K J 2007 *J. Mod. Opt.* **54** 1959
[2] Becker A, Dorner R and Moshammer R 2006 *J. Phys. B: At. Mol. Opt. Phys.* **38** S753
[3] Lambropoulos P 1985 *Phys. Rev. Lett.* **55** 2141
[4] Corkum P B 1993 *Phys. Rev. Lett.* **71** 1994
[5] Parker J S, Doherty B J S, Meharg K J and Taylor K T 2003 *J. Phys. B.: At. Mol. Opt. Phys.* **36** L393
[6] Prauzner J S *et al* 2007 *Phys. Rev. Lett.* **98** 203002
[7] Ruiz C, Plaja L, Roso L and Becker A 2006 *Phys. Rev. Lett.* **96** 053001
[8] Haan S L, Van J S Dyke and Smith Z S 2008 *Phys. Rev. Lett.* **101** 113001
[9] Lafon R *et al* 2001 *Phys. Rev. Lett.* **86** 2762
[10] Staudte A *et al* 2007 *Phys. Rev. Lett.* **99** 263002
[11] Rudenko A *et al* 2007 *Phys. Rev. Lett.* **99** 263003
[12] Kopold R, Becker W, Rottke H and Sandner W 2000 *Phys. Rev. Lett.* **85** 3781
[13] Feuerstein B *et al* 2001 *Phys. Rev. Lett.* **87** 043003
[14] Emmanouilidou A 2008 *Phys. Rev.* A **78** 023411
[15] Landau L D and Lifshitz E M 1977 *Quantum Mechanics* (New York: Pergamon)
Delone N B and Krainov V P 1991 *J. Opt. Soc. Am.* B **8** 1207
[16] Abrines R and Percival I C 1966 *Proc. Phys. Soc.* **88** 861
[17] Kustaanheimo P and Stiefel E 1965 *J. Reine Angew. Math.* **218** 204
[18] Smyth E S, Parker J S and Taylor K T 1998 *Comput. Phys. Commun.* **114** 1
[19] Parker J S, Doherty B J S, Taylor K T, Schultz K D, Blaga C I and DiMauro L F 2006 *Phys. Rev. Lett.* **96** 133001
[20] Emmanouilidou A and Staudte A 2009 *Phys. Rev.* A **80** 053415